

Research Paper

Numerical and experimental investigation of UV disinfection for water treatment



H.Y. Li ^{a,*}, H. Osman ^b, C.W. Kang ^a, T. Ba ^a

^a Institute of High Performance Computing (IHPC), Agency for Science, Technology and Research (A*STAR), 1 Fusionopolis Way, 16-16 Connexis, Singapore 138632, Singapore

^b Research & Development, Sembcorp Marine Ltd., Admiralty Road West, Singapore 759956, Singapore

HIGHLIGHTS

- UV irradiation for water treatment is numerically and experimentally investigated.
- Fluence rate E increases exponentially with the increase of UVT.
- UV dose distribution moves to a high range with increase of UVT and lamp power.
- A linear relationship is observed between fluence rate E and average UV dose D_{ave} .
- D_{ave} decreases with the increase of UVT and fluid flow rate.

ARTICLE INFO

Article history:

Received 22 January 2016

Revised 5 September 2016

Accepted 19 September 2016

Available online 20 September 2016

Keywords:

UV disinfection

UV reactor

Numerical simulation

UV dose

ABSTRACT

Disinfection by ultraviolet (UV) for water treatment in a UV reactor is numerically and experimentally investigated in this paper. The flow of water, UV radiation transportation as well as microorganism particle trajectories in the UV reactor is simulated. The effects of different parameters including UV transmittance (UVT), lamp power and water flow rate on the UV dose distribution and average UV dose are studied. The UV reactor performance in terms of average UV dose under these parameters is analysed. Comparisons are made between experiments and simulations on the average UV dose and reasonable agreement is achieved. The results show that the fluence rate increases exponentially with the increase of UVT. The UV dose distribution profiles moves to a high range of UV dose with the increase of UVT and lamp power. The increase of water flow rate reduces the average exposure time of microorganism particles to the UV light, resulting in the shifting of UV dose distribution to a low range of UV dose. A linear relationship is observed between fluence rate and the average UV dose. The average UV dose increases with the increase of lamp power while it decreases with the increase of UVT and water flow rate.

© 2016 Elsevier Ltd. All rights reserved.

1. Introduction

Ultraviolet (UV) disinfection is an effective way for water treatment [1]. The central idea of this method is to use UV-C, one range of wavelength from UV light, to inactivate microorganisms for functioning and reproducing itself. UV light is able to pass through the cell wall of the microorganisms and absorbed by the protein and nucleotides so that it can disrupt the structure of DNA or RNA of the microorganism. Unlike cryptosporidium for water treatment, UV disinfection for drinking water treatment does not introduce or generate any hazardous chemical materials or by-product during the procedure. Therefore, it grows rapidly since 1985 [2]. UV disinfection for water treatment becomes more

popular when the UV disinfection method was included in the Surface Water Treatment Rule by United States Environmental Protection Agency [3].

The UV disinfection system for water treatment generally consists of one or more UV lamps and a conduit or duct in which the water to be irradiated. Given the location of the UV lamps and water, UV reactors can be divided into two different types, i.e. contact and noncontact types [4,5]. Contact reactor is more popularly used. In the contact reactor, the lamps are enclosed by the cylindrical quartz sleeves. These quartz sleeves are used to separate the lamps from water. During the operation, water carried along suspended microorganisms into the reactor. These microorganisms absorb radiation during their transit in the reactor. Given the non-uniformity of the UV fluence rate field in the reactors, different microorganism absorbs different UV dose when it flows through the reactor. UV dose is the amount of UV energy per unit

* Corresponding author.

E-mail address: lih@ihpc.a-star.edu.sg (H.Y. Li).

Nomenclature

a	absorption coefficient (1/m)	\vec{u}	velocity vector (m/s)
c_1, c_2, c_3	constant	UVT	transmittance
$C_D, C_{1\varepsilon}, C_{2\varepsilon}$	constant	x, y, z	Cartesian coordinate
d_p	particle diameter (m)	<i>Greek symbols</i>	
D	UV dose (J/m ²)	μ	dynamic viscosity (kg/m s)
E	fluence rate (W/m ²)	σ	Stefan Boltzmann constant (W/m ² K ⁴)
F	force (N)	κ	kinetic energy (m ² /s ²)
\vec{g}	gravity vector (m/s ²)	ε	energy dissipation rate (m ² /s ³)
G_κ	production of turbulent energy (kg/m s ³)	$\sigma_\kappa, \sigma_\varepsilon$	empirical constant
I	radiation intensity (W/m ²)	ρ	density (kg/m ³)
L	length of reactor (m)	<i>Subscripts</i>	
n	refractive index	<i>ave</i>	average
N	number of microorganisms	<i>p</i>	particles
P	pressure (Pa)	<i>r</i>	reference
Q	flow rate (m ³ /s)	<i>t</i>	turbulent flow
Re	Reynolds number	<i>*</i>	dimensionless
\vec{s}	direction vector (m/s)		
t	time (s)		
T	temperature (°C)		

area that incident on a surface. Such UV dose absorbed by these microorganisms affects the performance of the reactor. Generally, an optimum UV dose can be calculated from the desired inactivation rate which is associated with the total and live microorganism before and after the reactor. The performance of a UV reactor is governed by many parameters including, among others, the reactor diameter, lamp arrangement, lamp power, fluid properties and fluid flow rate. Therefore, knowing the effects of these parameters on the performance of the UV reactor is important for designing an efficient UV reactor.

The performance of the UV reactor can be investigated experimentally. A detailed summary for experimental study of UV disinfection for water treatment can be found in the work of Hijnen et al. [1]. Generally, experimental study of UV reactor performance requires large scale test facility and expensive high-resolution equipment to provide convincing data. Besides, the operating cost of the UV reactor is substantial. Experimental study, although expensive, is still a desired and straightforward way to evaluate the performance of one UV reactor. Janex et al. [6] tested the effect of water quality and hydraulic characteristics on the performance of the UV reactor. They concluded that the performance of the UV reactor is affected by its geometry and the type of microorganism in the water. With the development of the dyed microspheres method [7], it makes the measurement of UV dose distribution in a UV reactor possible. This serves as potential evaluation platform for the UV reactor performance, leading to a better and more in-depth understanding of the UV reactor. Blatchley et al. [7] used the dyed microspheres to measure the UV dose distribution in a large scaled UV reactor. Their experimental results agreed well with their simulation results. Zhao et al. [8] used fluorescence microspheres to measure the UV dose distribution in a UV reactor. They investigated different orientations of the inlet pipe, i.e. straight and elbow inlet pipe on the UV dose distribution. They concluded that no significant difference is observed for different inlet pipe configurations.

Generally, the study of UV reactor is complex as it involves with fluid flow, UV radiation transport as well as microorganism movements. One of the important factors which affect the UV reactor performance is the flow path of the microorganisms. Fluid flow in the reactor is usually highly turbulent. It makes the trajectories of the microorganisms complex and unpredictable. In view of this, numerical simulations play an essential complementary role in

understanding various processes involved in the reactor. It can provide useful detailed insights. Numerical simulation of UV process in a reactor is extensively studied. Chiu et al. [9] numerically studied the effects of the reactor geometry on the UV dose distribution as well as microbial inactivation. They have evaluated the reactor with different side walls including wavy side wall and baffled side wall. The results showed that both of these two geometries have high UV dose distribution. A three-dimensional numerical model was built by Munoz et al. [10] to simulate the full scale UV reactor. They have investigated the sensitivity of particle numbers on the reduction equivalent dose (RED). RED is another factor which is used to evaluate the UV reactor performance. The model was applied to simulate different operating mode of the lamps as well as arrangements of the lamps and baffles. Their results showed that RED is very sensitive to the particle numbers injected into the reactor. Different reactor requires different number of particles to achieve a stable solution. In addition to the experimental study for the orientation of the inlet pipe on the UV dose distribution by Zhao et al. [8], they also performed numerical simulation to compare with their experimental data. Their numerical simulation predicted higher RED compared with experimental data. Xu et al. [11] developed a three-step UV fluence rate and fluid dynamics (TURF) model to simulate fluid flow, radiation and microorganism movements in the UV reactor. Their simulation is performed based on the commercial software of FLUENT ANSYS platform. The model was applied to study the effect of water flow rate, reactor size and shape as well as the lamp arrangements [12] on the UV reactor performance. The results showed that these parameters have complex effect on the microbial inactivation.

Although there exist extensive studies of UV disinfection for water treatment in the literature, however, the performance of a UV water treatment reactor is reactor, water content and operation condition specific. For example in terms of water content, even for the same reactor, the performance depends on both the type and quantity of the micro-organisms. Generalizing the findings from these studies for design and operation of a new reactor is therefore uncertain.

Given the wide range of possible water content and operation conditions, lab-scaled experimentation is expansive and time consuming. Besides, scaling-up the results of a lab-scaled experiment for use in an actual reactor is not straight forward. On the other hand, sole numerical study, though much less expensive, may

not capture the actual physics of the problem sufficiently and risky to be employed directly in actual engineering applications. A more conclusive study requires these two components complementing each other. However, complete combined experimental and numerical investigation is relatively scarce. The present work is undertaken to complement the existing literature.

Therefore, for a new UV water treatment reactor (lab-scaled, designed and commissioned in Singapore), the present study investigates its performance both experimentally and numerically. In the experimental study, the UV dose absorbed by the microorganisms in the reactor is measured. In the numerical study, ANSYS FLUENT with user-defined function (UDF) implemented in evaluating UV dose distribution is employed. The numerical model is validated using the experimental data (comparisons of both UV fluence rate and average UV dose). Then, parametric studies including UV transmittance (UVT), lamp power and water flowrate on the UV fluence rate, UV dose distribution and average UV dose, are performed. To the best knowledge of the authors, the above mentioned parameters critical in designing an efficient UV reactor, have not been conclusively studied using a combined experimental and numerical investigation. With the numerical model validated, it is then applicable to other similar scaled UV water treatment reactor even without additional experimentation. This could substantially save company's time and money in costly replication of the experimental tests.

2. Experiments

2.1. UV reactor

A UV reactor installed at Sembcorp Marine's test-bed facility is used as the physical system for model evaluation. The schematic diagram of the reactor under investigation is shown in Fig. 1. The reactor is a U-shaped design constructed from stainless steel. Two baffle plates were fixed to the internal walls of the reactor, one is positioned near the outlet and the other is at the longitudinal center of the reactor. Quartz sleeves are mounted onto the baffle plates such that the orientation is parallel to the flow. Besides functioning as support structures for the quartz-lamp assembly, the baffle plates also promote radial mixing. The quartz sleeves have length covering almost the entire length of the reactor. Each quartz sleeve houses a low-pressure amalgam lamp which emits

monochromatic radiation at germicidal wavelength of 253.7 nm. Quartz air gap of around 6 mm exists between the surface of the lamp and the internal surface of the quartz sleeves. A UV sensor constructed to the ONORM [13] standard and is positioned to measure fluence rate at a point approximately 10 mm from the surface of the quartz in the radial direction. Thus the measured fluence rate is primarily due to the radiation from the lamp closest to the sensor window; contribution from adjacent lamps is found to be negligible. The experiments were carried out using new lamps to ensure uniform radiation flux on all lamps. A flow meter and two pressure gauges with analogue outputs were installed at connecting spools at the inlet and outlet of the reactor. A portable UVT meter is also used to calibrate the water at specific UVTs.

2.2. Experimental procedure

Fig. 2 shows the schematic diagram of the experimental system. Water of variable UVT is prepared by first filling a dosing tank with freshwater. Sodium thiosulfate is then added and mixed well until the desired UVT is obtained. UVT of the solution is measured using portable UVT meter calibrated with deionized water. Water from the dosing tank is then transferred to the UV reactor using a centrifugal pump until the reactor is full and all lamps are fully submerged. The lamps are then switched on and fluence rate measurement from the installed UV sensor is recorded when the fluence rate has stabilized. The process is repeated for different UVT and radiant power. Lamp radiant power is adjusted by controlling the voltage supplied to the lamps through the ballasts. In these experiments, challenge microorganisms are introduced at the upstream of the UV reactor. Measurement of UV dose is carried out by biosimetry technique involving the application of MS2 bacteriophage. In this method, the dose-response curve ($\log N/N_0$ vs. fluence) for MS2 is first developed using a bench-scale collimated beam experiment. Next, a full-scale reactor testing was carried out by injecting MS2 at the inlet of the UV reactor. The bacterial diameter injected in the fluid ranged from 10 to 50 μm and the concentration of bacterial particles is 3000 per cubic meters. The log inactivation was determined by measuring the MS2 concentration at the influent and the effluent of the reactor. By passing the biosimulator into the reactor, and obtaining concentration of viable MS2 before and after the reactor, the fluence of the reactor for the particular power setting and flow rate can be determined using the calibration curve obtained previously.

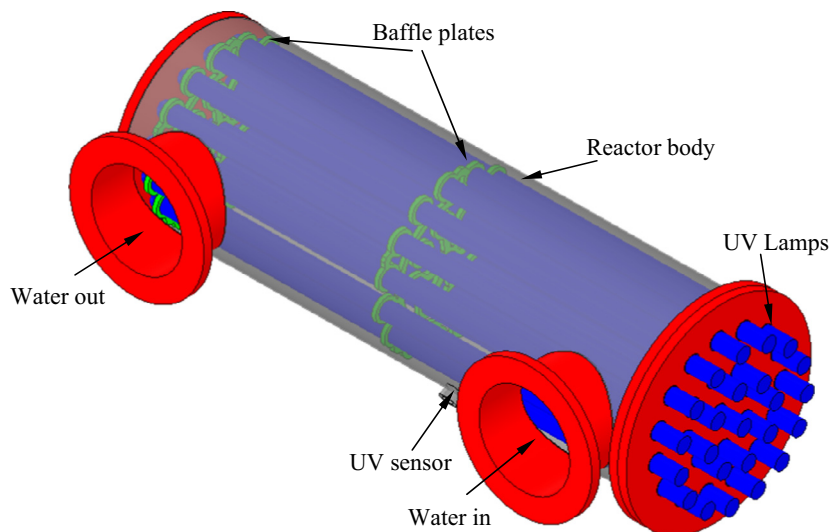


Fig. 1. The schematic diagram of the UV reactor.

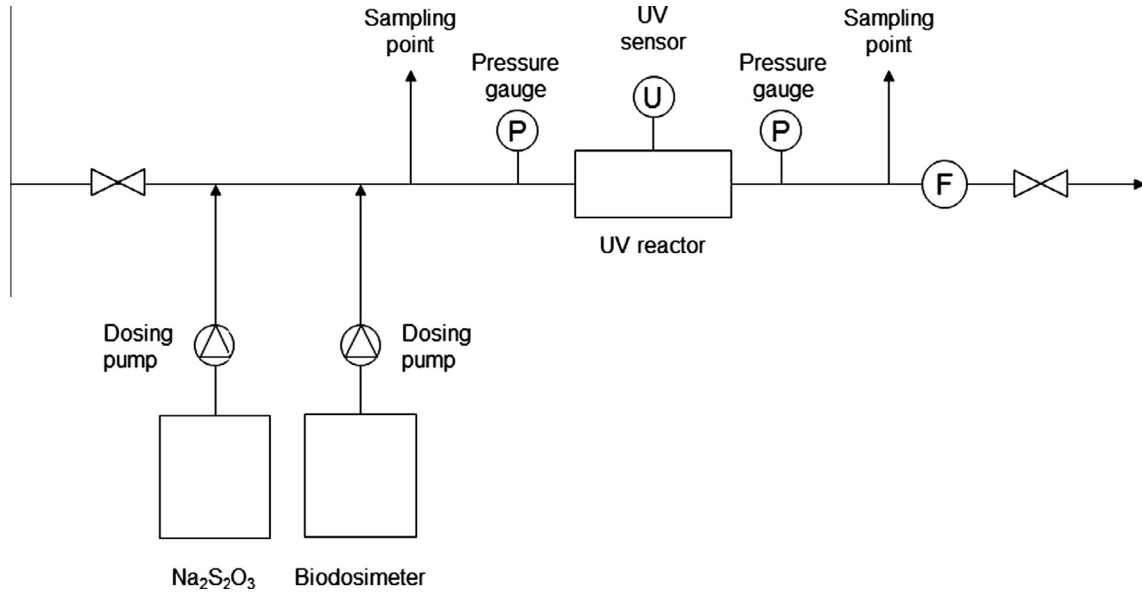


Fig. 2. The schematic diagram of the experimental set-up.

2.3. Uncertainty analysis

There are two groups of uncertainties for the measured data, i.e. random uncertainties and systematic uncertainties. Systematic uncertainties can be minimized with careful treatment while random uncertainties generally caused by unknown and unpredictable changes in the experiment. Therefore, it cannot be avoided. The uncertainties of pressure, flow rate and UV fluence rate are 2.0%, 0.12% and 3.0%, respectively. The uncertainty of UV dose is determined by the method proposed by Taylor [14]. If x, \dots, y, \dots, z are measure quantities with uncertainties $\delta x, \dots, \delta y, \dots, \delta z$ and these measure values are used to get the function of e . Then the uncertainty in e is

$$\delta e = \sqrt{\left(\frac{\partial e}{\partial x} \delta x\right)^2 + \dots + \left(\frac{\partial e}{\partial y} \delta y\right)^2 + \dots + \left(\frac{\partial e}{\partial z} \delta z\right)^2} \quad (1)$$

It is assumed that the uncertainties of the measured data in the current work are independent and random with normal distribution. Based on Eq. (1), the uncertainty of the UV dose is calculated to be 6.3%.

3. Numerical simulation

3.1. Problem description

Numerical study of UV reactor involves with simulation of water flow, radiation transport and microorganism trajectories in the reactor. Water carried along suspended microorganisms into the reactor. With the UV lamps switched on, the microorganism absorbs UV dose along its flow path. Given the non-uniform distribution of UV intensity (UVI) as well as the different flow path of the microorganism, the fluence rate hitting on each microorganism is different. Therefore, UV dose absorbed by each microorganism is also different. The simulation in this paper is to predict the UV dose for different microorganisms. Note that the lamps and baffle plates are not included in the simulation while their walls are kept. The inlet pipe and outlet pipe have been extended for another 5 times of the diameter to minimize the effect of boundary conditions in the simulation.

3.2. Governing equations

As mentioned before, the current simulation involves with water flow, radiation transport as well as microorganism particle tracking. The problems are then governed by Navier-Stokes equation with proper turbulent flow model, discrete ordinates (DO) radiation model [15] as well as discrete phase model (DPM) in the FLUENT manual [16].

The conservation equations governing the transport of mass, momentum with considering turbulent flow are given by

$$\nabla \cdot (\rho \vec{u}) = 0 \quad (2)$$

$$\nabla \cdot (\rho \vec{u} \vec{u}) = -\nabla P + \nabla \cdot [(\mu + \mu_t)(\nabla \vec{u} + \nabla \vec{u}^T)] - \nabla \cdot \left(\frac{2}{3} \rho k \vec{I}\right) \quad (3)$$

where k is the turbulent kinetic energy per unit mass. For the case considering turbulent flow, κ - ϵ model [17] is adopted as it has been well validated by researchers for simulation of fluid flow in reactor through the comparison with their experimental results [18,19]. This model is also widely used by many researchers such as Lyn et al. [20], Munoz et al. [10] and Zhao et al. [8], to name a few. The equations for solving κ and ϵ are:-

$$\nabla \cdot (\rho \vec{u} \kappa) = \nabla \cdot \left(\frac{\mu_t}{\sigma_\kappa} \nabla \kappa\right) + G_\kappa - \rho \epsilon \quad (4)$$

$$\nabla \cdot (\rho \vec{u} \epsilon) = \nabla \cdot \left(\frac{\mu_t}{\sigma_\epsilon} \nabla \epsilon\right) + \frac{\epsilon}{K} (C_{1\epsilon} G_\kappa - C_{2\epsilon} \rho \epsilon) \quad (5)$$

where $C_{1\epsilon}$, and $C_{2\epsilon}$ are the constants with values of 1.44 and 1.92, respectively. σ_κ and σ_ϵ are 1.00 and 1.3, respectively [21]. G_κ is the production of turbulence kinetic energy. The eddy viscosity μ_t is expressed as:

$$\mu_t = \rho C_\mu \frac{\kappa^2}{\epsilon} \quad (6)$$

C_μ is equal to 0.09.

The DO model considers the radiative transfer equation is written as:

$$\nabla \cdot (I \cdot \vec{s}) + aI = an^2 \frac{\sigma T^4}{\pi} \quad (7)$$

where a is the absorption coefficient, n is the refractive index. σ is Stefan-Boltzmann constant. I is the UV intensity and T is the temperature.

The trajectory of the microorganism particles was predicted through the integration of the force balance on the particles based on the Lagrangian reference frame [22]. The mathematical formulation for particle movement is [23]:

$$\frac{d\vec{u}_p}{dt} = F_D(\vec{u}_p - \vec{u}) + \frac{\vec{g}(\rho_p - \rho)}{\rho_p} + \vec{F} \quad (8)$$

The subscript p represents the microorganism particles. u_p and u are the microorganism particle and water velocity, respectively. F_D is the drag force exerted on water by the microorganism particle [16]. \vec{F} is the other forces involved such as virtual force and pressure gradient force. The mathematical expression of F_D is [16]:

$$F_D = \frac{18\mu}{\rho_p d_p^2} + \frac{C_D Re}{24} \quad (9)$$

where C_D is the drag force coefficient and Re is the Reynolds number. d_p is the microorganism particle diameter. The expression for C_D [23] and Re are, respectively:

$$C_D = c_1 + \frac{c_2}{Re} + \frac{c_3}{Re^2} \quad (10)$$

$$Re = \frac{\rho d_p |\vec{u}_p - \vec{u}|}{\mu} \quad (11)$$

c_1 , c_2 and c_3 are constants which can be applied for spherical particles for all ranges of Re [23]. The expressions of these constants are:

$$c_1, c_2, c_3 = \begin{cases} 0, 24, 0 & 0 < Re < 0.1 \\ 3.69, 22.73, 0.0903 & 0.1 < Re < 1 \\ 1.222, 29.1667, -3.8889 & 1 < Re < 10 \\ 0.6167, 46.5, -116.67 & 10 < Re < 100 \\ 0.3644, 98.33, -2778 & 100 < Re < 1000 \\ 0.357, 148.62, -47,500 & 1000 < Re < 5000 \\ 0.46, -490.546, 578,700 & 5000 < Re < 10,000 \\ 0.5191, -1662.5, 5416,700 & Re \geq 10,000 \end{cases} \quad (12)$$

In this study, the virtual force and the force incurred by the pressure gradient is included. The mathematical formulation for the combination of these two forces is [16]:

$$\vec{F} = 0.5 \frac{\rho}{\rho_p} \frac{d(\vec{u} - \vec{u}_p)}{dt} + \frac{\rho}{\rho_p} \vec{u} \nabla \cdot \vec{u}_p \quad (13)$$

3.3. Solution procedure

The procedure for simulating of the current problem is divided into three different steps based on the model used for solving different problems. These are:

- (1) Simulation of water flow in the reactor.

In this simulation, steady state simulation is performed. SIMPLE method is adopted to deal with the coupling of the pressure and velocity [24,25]. The second order upwind scheme is used to deal with the convection term in the N-S equation. The first order

upwind scheme is used for the convection term in both the turbulent kinetic energy equation and dissipation equation.

A uniform velocity is used at the inlet boundary and a constant pressure is used at the outlet boundary. Such pressure value is obtained from the experimental data. The walls are assumed to be no-slip.

- (2) Simulation of radiation heat transfer in the reactor.

With the converged flow field obtained above, the radiation transport equation is solved in this step. A constant radiation flux boundary condition is used for all the lamp walls. The rest walls including the reactor wall and baffle walls are assumed to be opaque. As the flow in the reactor is highly turbulent, the temperature increase caused by the UV lamps is generally low due to the high convection heat transfer. Through the order-of-magnitude analysis, the temperature difference between the lamps and the fluid is around 0.1 °C. Therefore, the radiation caused by the temperature difference among different materials in the reactor can be neglected. Prior to performing the radiation heat transfer simulation, the flow field is patched to 1 K to minimize the temperature effect on the radiation field.

- (3) Particle trajectory simulation.

In this step, the movements of the microorganism particles under the converged flow and radiation fields are simulated. The microorganism particles are injected through the inlet boundary with the injection files. These microorganism particles flow out of the reactor through the outlet boundary. The diameter of these microorganism particles is assumed to be 30 μm. The walls are set to be reflected with no energy loss occurred when microorganism particles collided with walls. The initial velocity of the microorganism particles is set to be 0. One way coupling is used as the volume fraction of the microorganism particles is quite small. The discrete random walk model is activated to account for the random effects of turbulence on the trajectories of the microorganism particles [26].

3.4. Numerical errors

There are two major sources of numerical error which is related to the numerical integration scheme for the equations, i.e. truncation error and round-off error. The truncation error is caused by the omission of high order terms during Taylor expansion. The round-off error η of the Linux workstation used in the simulation is 10^{-12} . The total numerical error is approximately:

$$\varepsilon \sim \frac{\eta}{h} + h \quad (14)$$

where h is the maximum grid size used in the simulation. It is obvious that the grid size is the dominant numerical error. Such maximum and minimum grid sizes in the medium mesh are around 0.01 m and 0.002 m, respectively. Therefore, the maximum and minimum numerical errors are around 1% and 0.2%, respectively. This numerical error applies to all the simulation cases performed in this paper.

4. Results and discussion

4.1. Mesh and particle number sensitivity study

For the ease of discussion, the dimensionless quantities are used based on the corresponding reference values. These reference values include u_r , t_r , Q_r , E_r and D_r . The subscript r represents reference. u_r is the inlet velocity at water flow rate of 0.14 m³/s.

Q_r is water flow rate which is chosen to be $0.14 \text{ m}^3/\text{s}$. t_r is defined as:

$$t_r = \frac{L}{u_r} \tag{15}$$

where L is the length of the reactor. E_r is the radiation intensity at lamp wall under 100% power. D_r is obtained from the following equation:

$$D_r = E_r \times t_r \tag{16}$$

The dimensionless pressure drop is chosen to be:

$$P^* = 2\Delta P / \rho u_r^2 \tag{17}$$

Prior to the case study, mesh and particle sensitivity study is performed. Three different mesh sizes have been tested. The numbers of elements after converting to polyhedral mesh in ANSYS FLUENT are 1.48 million, 2.92 million and 4.23 million, respectively. They are called coarse mesh, medium mesh and fine mesh thereafter. Boundary layers are used near the walls. y^+ values for the reactor wall under coarse, medium and fine meshes are 78.2, 59.33 and 52.41, respectively. y^+ values for the lamp wall under coarse, medium and fine meshes are 51.4, 40.64 and 37.64, respectively.

Table 1 shows the dimensionless pressure drops under different mesh sizes at $Q/Q_r = 0.96$. Such pressure drop is taken from pressure difference between the inlet and outlet boundaries. It is seen that the dimensionless pressure drop between medium mesh and fine mesh is close to each other.

Comparisons of the radiation field on E/E_r under different UVT among the three mesh sizes are shown in Fig. 3. UVT is the measure of UV energy at a particular wavelength or frequency which is actually transmitted through water from the UV lamp. The higher the UVT, the more energy is transmitted through water to the microorganisms. UVT is associated with the water absorption coefficient a .

Table 1
Dimensionless pressure drops under different mesh sizes at $Q/Q_r = 0.96$.

	Coarse mesh	Medium mesh	Fine mesh
P^*	2.0	1.90	1.89

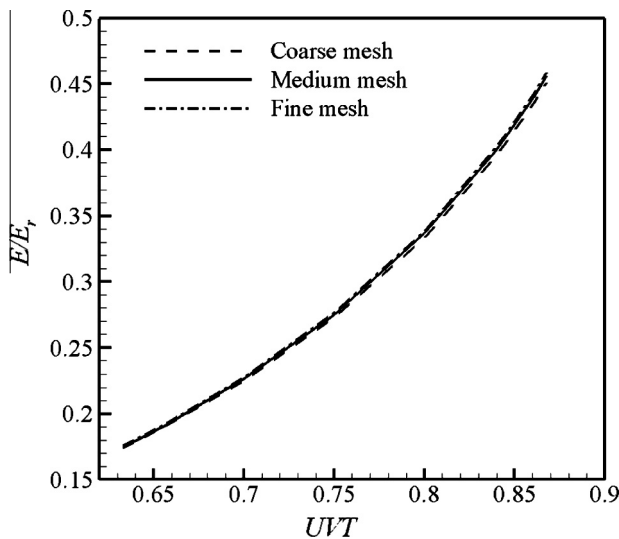


Fig. 3. Comparison of E/E_r vs. UVT under different mesh sizes.

Mesh sensitivity study is performed to compare E/E_r on the UV sensor surface. Fluence rate E is the UV intensity hitting on the solid surface. Fig. 3 shows the variation of E/E_r under the three meshes while E_r is the radiation intensity at the lamps wall. It is observed that E/E_r is not sensitive to the mesh. The largest difference of E/E_r between medium mesh and fine mesh is 0.6% while the largest difference between medium mesh and coarse mesh is 1.1%. Therefore, the medium mesh size is enough for simulation of both water flow and radiation field.

The effect of particle numbers on the UV dose distribution based on medium mesh size is compared. UV dose is defined as the integration of fluence rate E over time. Fluence rate represents the incident radiation from the UV lamps to the microorganism particles. The mathematical expression for UV dose is:

$$D = \int_0^t E dt \tag{18}$$

Four different microorganism particle numbers are tested to produce sufficient accuracy in calculation of UV dose. These are 1000, 5000, 10,000 and 15,000. The method in determining the number of particles is proposed by Graham and Moyeed [27]. It is known that use of less particles will result in a poor accuracy and low statistical insignificance while use of a large number of particles results in unnecessary computational effort.

Fig. 4 shows the dimensionless UV dose distribution under different particle numbers. The normalized frequency f represents the particle percentage. It is obvious the UV dose distribution between 10,000 microorganism particles and 15,000 microorganism particles are close to each other. Examination on the average UV dose for different particle numbers was further carried out. The average UV dose is an important factor which reflects the UV reactor performance. It is calculated by:

$$D_{ave} = \sum_{i=0}^{i=N_p} N_i D_i / N_p \tag{19}$$

where D_{ave} is the average UV dose. N_i is the number of microorganism particles which absorbed UV dose of D_i . N_p is the total number of microorganism particles in the UV reactor. The results showed that the difference for the average UV dose between 10,000 particles and 15,000 particles is only 0.5% while the difference between 10,000 microorganism particles and 5000 microorganism particles, 5000 microorganism particles and 1000 microorganism particles are 4% and 8%, respectively. Therefore, 10,000 particles are sufficient to get a stable solution in the current work. Such numbers will be used in the following simulations.

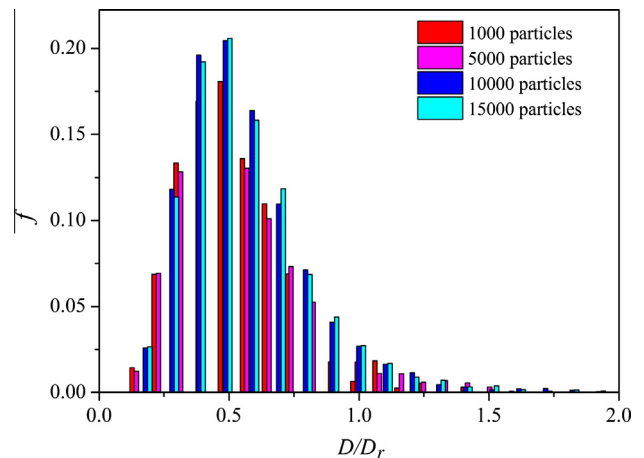


Fig. 4. Comparison of particle numbers on D/D_r , based on the medium mesh.

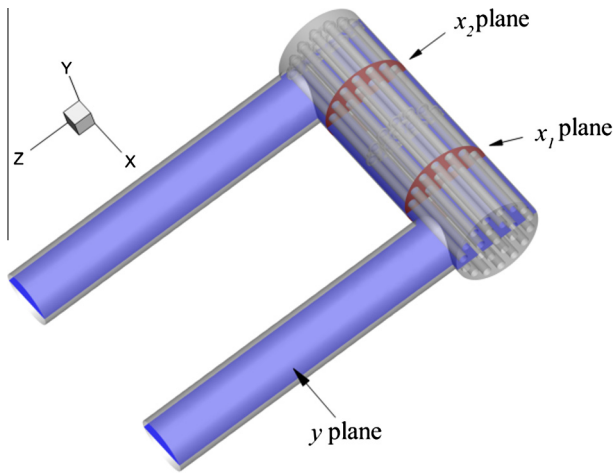


Fig. 5. Schematic diagram of the cutting planes.

4.2. Water flow and radiation fields

In order to show the flow and radiation distributions in the reactors, different cutting planes are selected. These cutting planes are shown in Fig. 5. y cutting plane is chosen to cross the centerline of the inlet pipe, outlet pipe and the reactor. Two x cutting planes, i.e., x_1 and x_2 represent two different locations. These locations are chosen to show the flow and radiation features for water before and after passing through the baffle plate, respectively.

Fig. 6 shows the dimensionless velocity distribution at the selected cutting planes. Generally, water flow in the reactor is complex and highly turbulent given the existence of the lamps. Seen from Fig. 6(a), it is interesting to find that the flow is divided into two streams when it flows to the outlet. One stream with high velocity flows directly to the outlet while the other stream forms a recirculation flow at the corner between the outlet pipe and the reactor. Given the inertial force, most of the fluid flows to the outlet pipe, leading to a high velocity. The fluid with high velocity and the fluid with low velocity at the corner form the recirculation

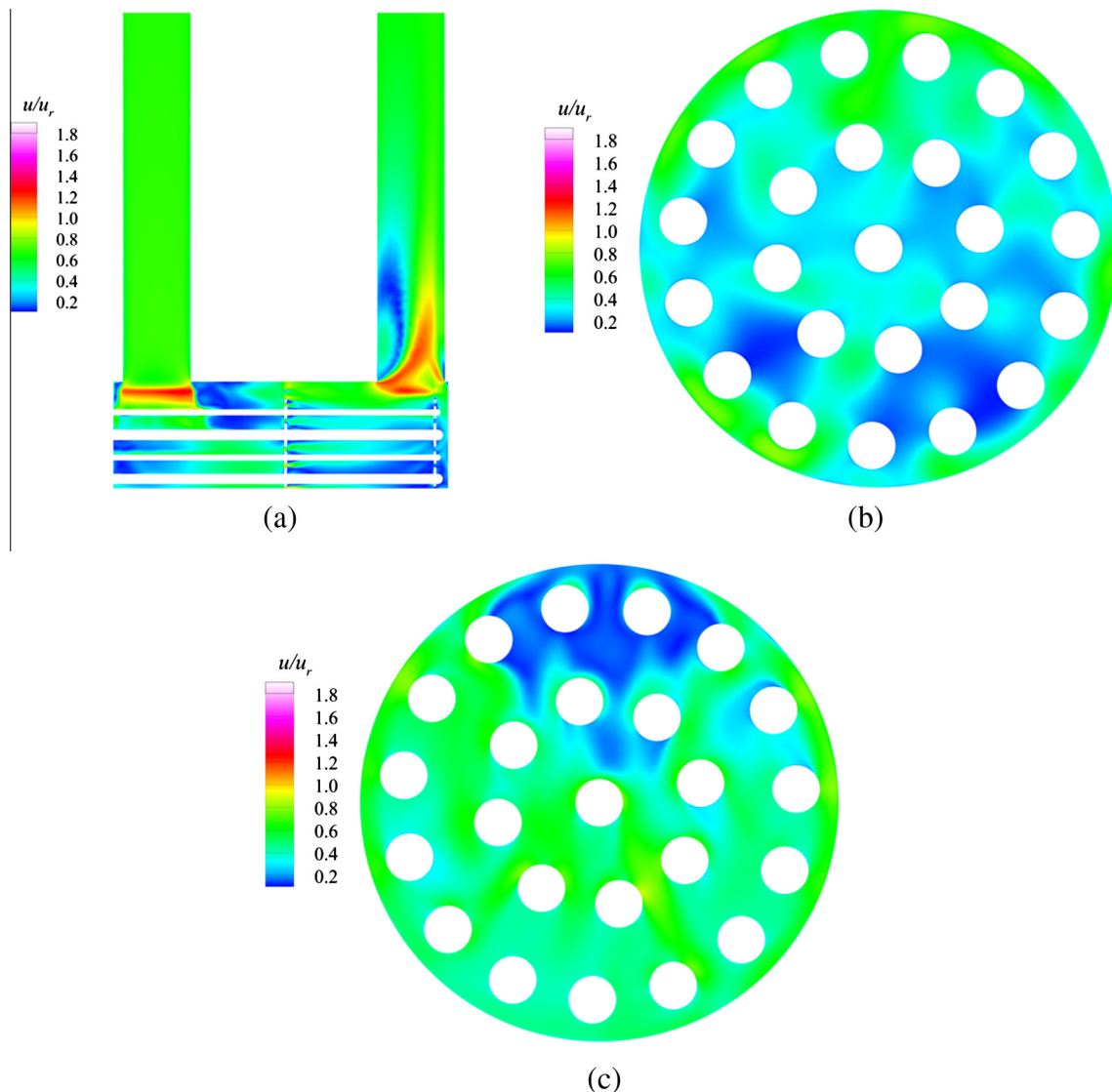


Fig. 6. u/u_r at (a) y , (b) x_1 and (c) x_2 cutting planes.

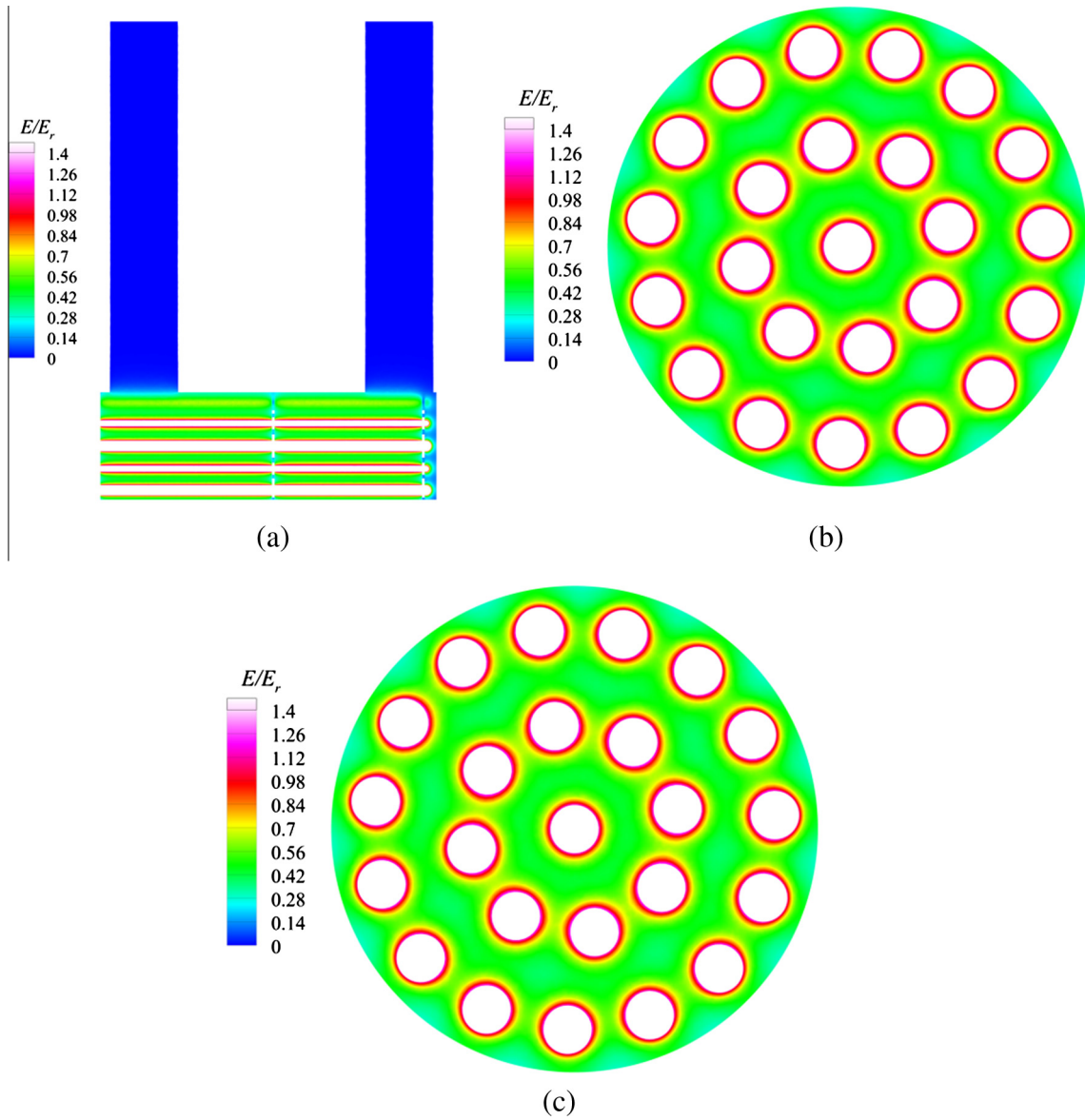


Fig. 7. E/E_r distribution at (a) y , (b) x_1 and (c) x_2 cutting planes.

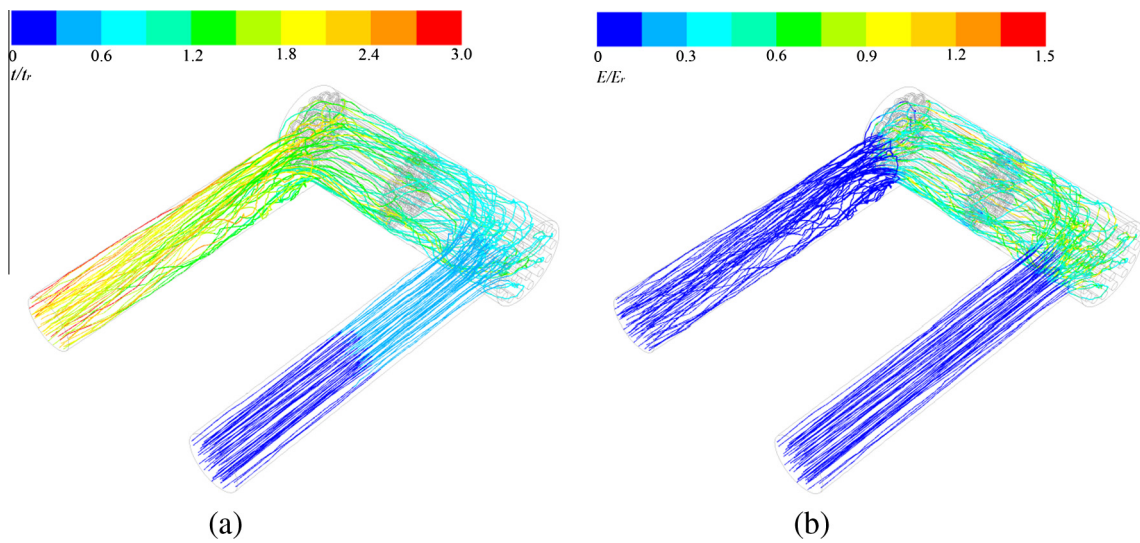


Fig. 8. Microorganism flow path colored by (a) t/t_r , and (b) E/E_r . (For interpretation of the references to colour in this figure legend, the reader is referred to the web version of this article.)

flow. Seen from the velocity distribution at different x -cutting planes, it is found that the flow field becomes relatively uniform after passing through the baffle plate. The low velocity at x_2 cutting plane (Fig. 6c) is caused by the existence of the outlet pipe ahead.

The dimensionless fluence rate E/E_r distribution at y -cutting plane is shown in Fig. 7(a). Fluence rate is dependent on the lamp power, lamp location and the water absorption coefficient. However, it is independent of water velocity. The high fluence rate occurs at the lamps walls as expected. With the increase of distance away from the lamps, the fluence rate decreases. Such variation trend can be clearly observed from E/E_r distribution at x_1 and x_2 planes in Fig. 7(b) and (c), respectively. These two figures have similar E/E_r distribution due to the same arrangement of the lamps. Shown by Fig. 7(a), the dimensionless fluence rate in the inlet and outlet pipes are almost 0. Therefore, it is assured that the extension of the 5 diameters of the domain has no effect on the simulation results for the radiation field.

Fig. 8(a) and (b) shows the selected microorganism particle trajectories colored by the dimensionless microorganism particle

resident time and fluence rate, respectively. Generally, the microorganism particle trajectories in the reactor are complex due to the arrangement of lamps and the baffle plates. It is hoped that these microorganism particles can stay in the reactors for a long time so that the exposure time of microorganism particles to the UV light is sufficient to destroy DNA and RNA. The microorganism particle trajectories colored by E/E_r show clearly the difference of radiation absorbed by different microorganism particles.

The variation of P^* under Q/Q_r is shown in Fig. 9. The increase of water flow rate increases the pressure drop in the reactor as expected. It is necessary to mention that the pressure drop is taken from two points which are 5 times diameter away from the inlet and outlet boundaries, respectively. These two points are the pressure sensor locations in the experimental setup. Generally, the simulation results agree reasonable with the experimental data.

UVT is inverse exponentially proportional to water absorption coefficient a . The higher the UVT, the lower the a . A low a indicates a less fluence rate absorbed by water. Therefore, the fluence rate irradiated to the microorganism increases. Fig. 10 shows the effects

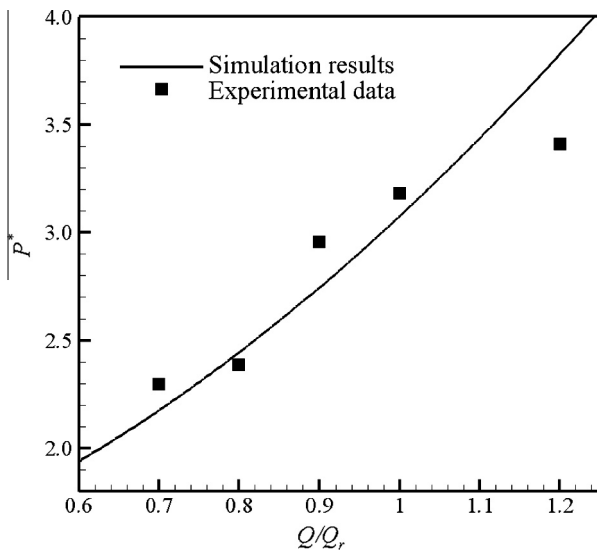


Fig. 9. Variation of P^* under different Q/Q_r in the reactor.

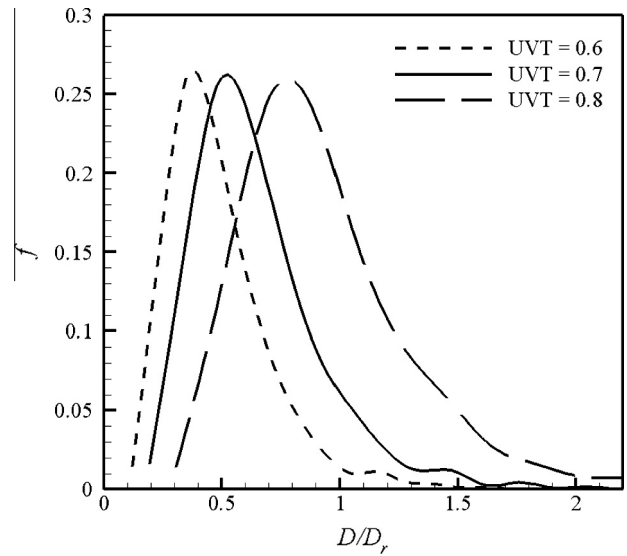


Fig. 11. Effect of UVT on D/D_r under 100% power.

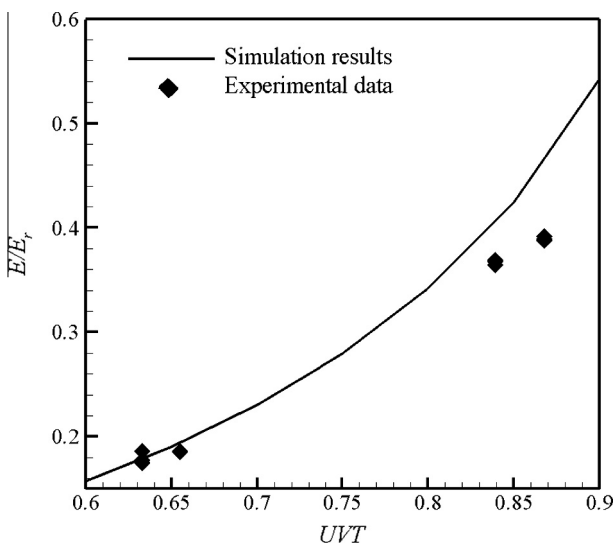


Fig. 10. Variation of E/E_r under different UVT in the reactor.

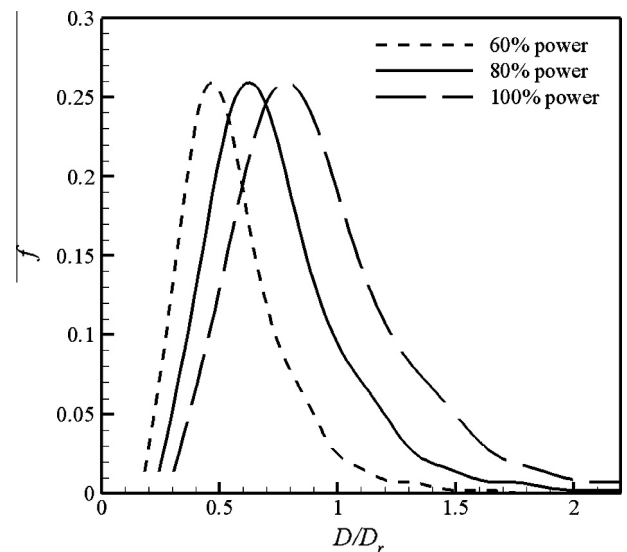


Fig. 12. Effect of lamp power on D/D_r distribution under 0.8 UVT.

of UVT on E/E_r in the reactor. Fluence rate increases exponentially with the increase of UVT. This fluence rate is measured by the UV sensor at the UV sensor location as showed in Fig. 1. Reasonable agreement is achieved between the simulation and experimental results.

4.3. UV dose distribution

Fig. 11 shows the effects of UVT on the dimensionless UV dose distribution D/D_r . UVT is an important parameter which reflects the quality of water. Generally, solid particles in water reduce UVT significantly. The performance of the UV reactor is highly dependent on UVT, i.e. the quality of water being treated. Seen from the graph, UV dose distribution moves to a high UV dose direction with the increase of UVT. This indicates that microorganism particles absorb more UV dose at high UVT than that of low UVT, leading to a better performance of the UV reactor. Of particular interests of this result is that it reflects the importance of

removing the solid particles prior to UV disinfection. These solid particles not only can reduce water UVT, but also deposit on the quartz sleeves which results in the reduction of transmittance of UV light from lamps to the microorganism particles.

Another important factor which affects the UV reactor performance is the lamp power. The dimensionless UV dose distribution D/D_r under different lamp power in the reactor is shown in Fig. 12. It is obvious that D/D_r shifts to a high range of UV dose with the increase of lamp power. This implies that the high UV dose is absorbed by the microorganism particles at high lamp power, showing a better performance of the reactor.

Fig. 13(a) shows the effect of water flow rate on D/D_r distribution. Increase of water flow rate increases water velocity which decreases the microorganism resident time in the reactor. Under such a condition, the exposure time for microorganism under UV light decreases. Therefore, the UV reactor performance reduces. As seen from the figure, the UV dose distribution shifts to the low range of UV dose at high water flow rate. An obvious difference was found for Q/Q_r between 0.8 and 1.0 while the difference between water flow rate ratio of 1.0 and 1.2 is not significant. With different profiles of UV dose distribution under different flow rates, it is indicated that the microorganism flow path under different flow rates are different. UV dose is associated with the fluence rate and the resident time of microorganism particles in the reactor. As the fluence rate is independent of flow rate, therefore, the difference of UV dose under different flow rate is mainly caused by the resident time of microorganism particle as well as its flow path. Fig. 13(b) shows the resident time of microorganism particles under different water flow rates. The resident time of microorganism particles is showcased with the dimensionless minimum resident time, maximum resident time and average resident time, respectively. The minimum and maximum resident time represent the time which the microorganism particles have the highest and lowest velocity in the reactor, respectively. The minimum and average resident time decreases linearly with the increase of water flow rate. While the maximum resident time decreases slightly before $Q/Q_r = 0.9$. After that, it decreases rapidly until the water flow rate reaches around $Q/Q_r = 1.05$. No significant decrease is found for the maximum resident time when the flow rate increases further.

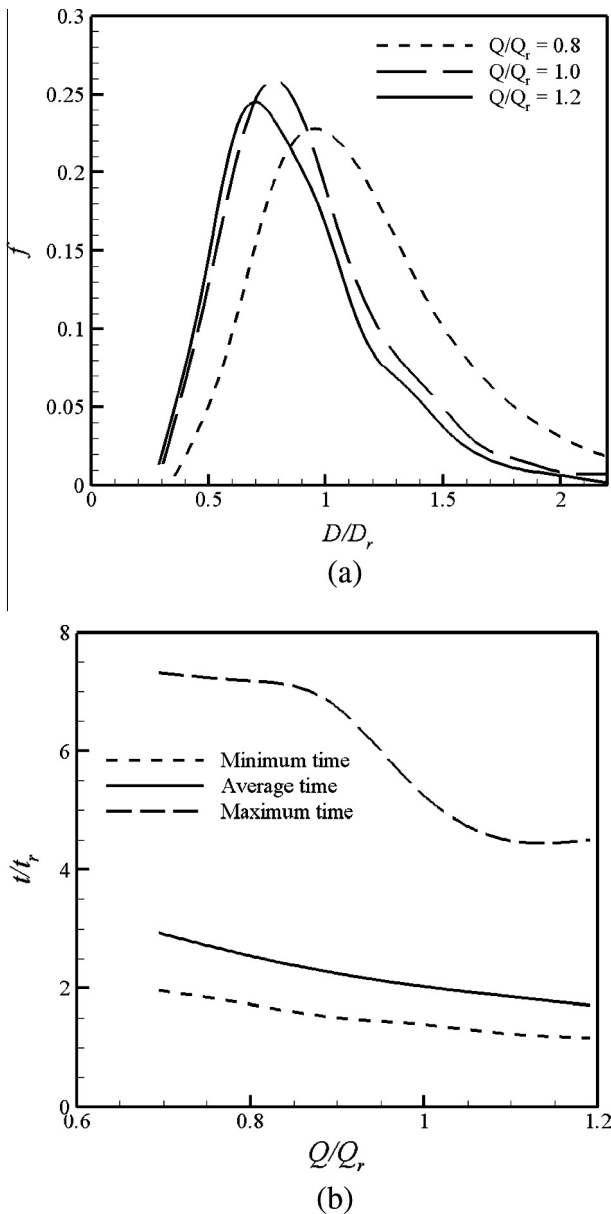


Fig. 13. Effect of Q/Q_r on (a) D/D_r , and (b) t/t_r under 0.8 UVT.

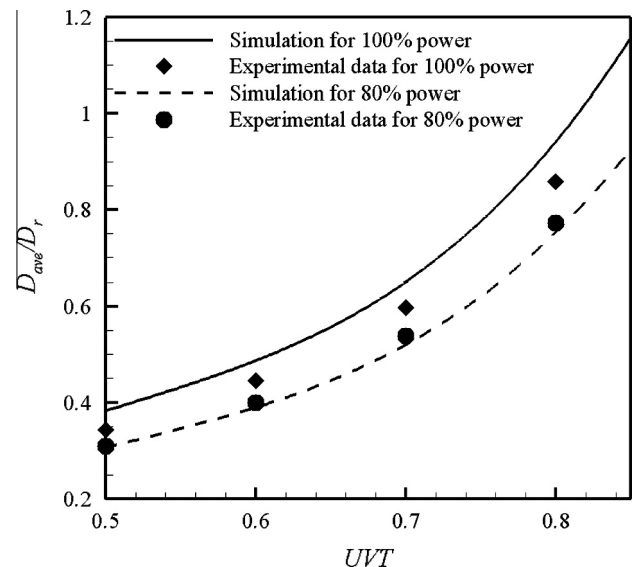


Fig. 14. Effect of UVT on D_{ave}/D_r for different lamp power.

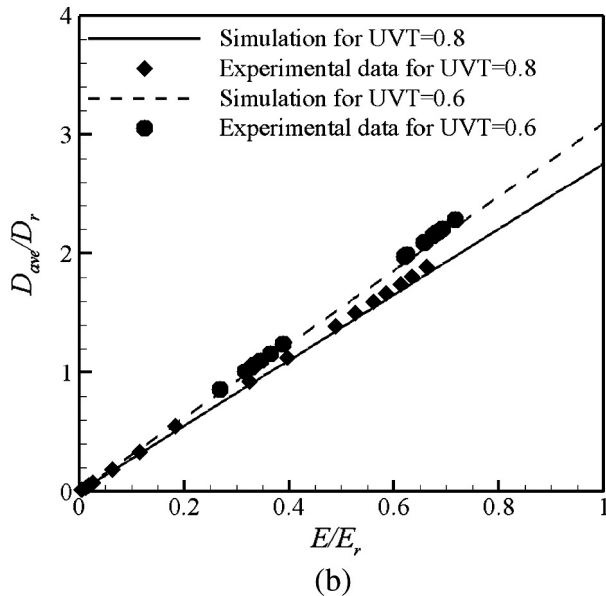
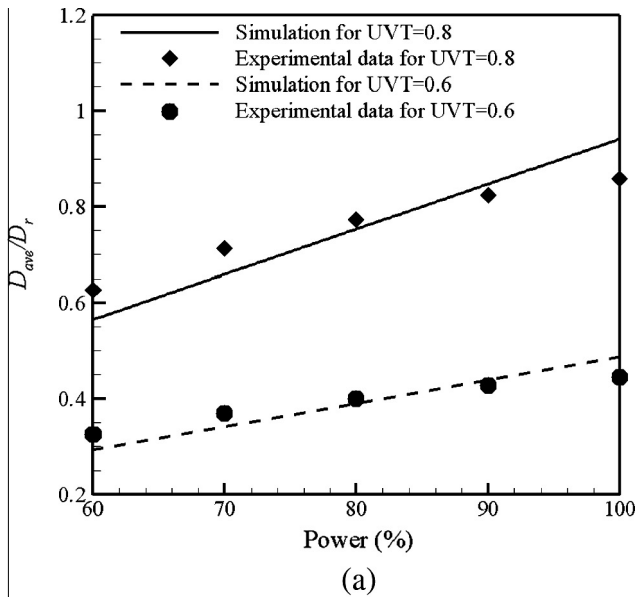


Fig. 15. Effect of (a) lamp power, and (b) E/E_r on D_{ave}/D_r for different UVT.

4.4. Average UV dose

Fig. 14 shows the effect of UVT on D_{ave}/D_r under 100% and 80% lamp power at water flow rate ratio of $Q/Q_r = 1$. D_{ave}/D_r increases exponentially with the increase of UVT under the two testing lamp powers. Higher lamp power gives larger D_{ave}/D_r as expected. The numerical simulation produces slightly higher D_{ave}/D_r compared with experimental data at 100% lamp power. While the simulation results agree well with the experimental data at 80% lamp power.

The effect of lamp power on the D_{ave}/D_r is shown in Fig. 15(a). Two different UVT, i.e. 0.6 and 0.8 are simulated at $Q/Q_r = 1.0$. It is seen that D_{ave}/D_r increases linearly with the increase of lamp power. The higher the UVT, the larger the D_{ave}/D_r . Generally, the simulation results agree reasonably with the experimental data except for the lowest and highest lamp power. Fig. 15(b) shows the variation of E/E_r with D_{ave}/D_r at $Q/Q_r = 1.0$. Seen from the graph, D_{ave}/D_r shows a linear increase with the increase of E/E_r . It is surprised to find that a slightly lower D_{ave}/D_r is obtained at 0.8 UVT compared with 0.6 UVT at the same E/E_r . This is different from

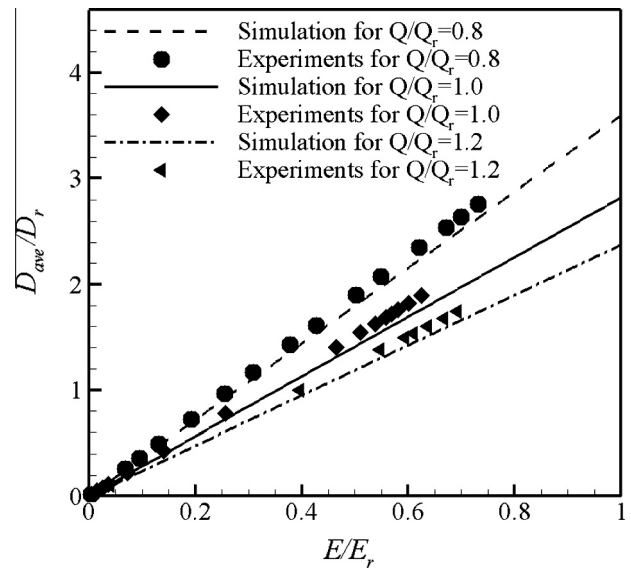


Fig. 16. Effect of Q/Q_r on D_{ave}/D_r for 100% lamp power and 0.7 UVT.

what observed in Fig. 15(a). High lamp power is required under low UVT as more energy is absorbed by water to achieve the same E as that of high UVT. While a high lamp power results in a high D_{ave}/D_r . Therefore, D_{ave}/D_r increases slightly under low UVT.

The effect of water flow rate on D_{ave}/D_r is shown in Fig. 16 under 100% lamp power and 0.7 UVT. As discussed before, the increase of water flow rate decreases the exposure time of microorganisms to the UV light. Therefore, D_{ave}/D_r reduces correspondingly at high water flow rate. D_{ave}/D_r shows a linear increase with the increase of E/E_r at different water flow rates. Generally, the simulation results agree well with the experimental data.

5. Concluding remarks

UV disinfection for water treatment in a UV reactor is studied in this paper. The effects of different parameters including UVT, lamp power and fluid flow rates on the UV dose distribution as well as the average UV dose are thoroughly investigated combined experimental and numerical study. Comparisons between numerical and experimental results under these parameters show reasonable agreement. The results of these critical parameters studied on the UV reactor performance in this paper can provide useful insights for the designing of an efficient UV reactor. With the numerical model validated, it can be used as guidelines for designing and evaluation of other scaled UV reactors without further experimentation. This could save time and money substantially in replication of the experimental tests for the company.

References

- [1] W.A.M. Hijnen, E.F. Beerendonk, G.J. Medema, Inactivation credit of UV radiation for viruses, bacterial and protozoan (oo)cysts in water: a review, *Water Res.* 40 (2006) 3–22.
- [2] N.F. Gray, *Microbiology of Waterborne Diseases Microbiological Aspects and Risks*, Waltham, MA, USA, 2014, pp. 617–630.
- [3] USEPA, Long Term 2 Enhanced Surface Water treatment Rule (LT2) Available from <http://water.epa.gov/lawsregs/rulesregs/sdwa/lt2/index.cfm>2006.
- [4] USEPA, Wastewater Technology Fact Sheet Ultraviolet Disinfection, EPA 832-F-99-064 http://water.epa.gov/scitech/wastetech/upload/2002_06_28_mtb_uv.pdf1999.
- [5] A.K. Ray, Design, modelling and experimentation of a new large-scale photocatalytic reactor for water treatment, *Chem. Eng. Sci.* 54 (1999) 3113–3125.
- [6] M.L. Janex, P. Savoye, Z. Do-Quang, E.R. Blatchley III, J.M. Lainé, Impact of water quality and reactor hydrodynamics on wastewater disinfection by UV, use of

- CFD modelling for performance optimization, *Water Sci. Technol.* 38 (1998) 71–78.
- [7] E.R. Blatchley III, C. Shen, Z. Naunovic, L. Lin, D.A. Lyn, J.P. Robinson, K. Ragheb, G. Grégori, D.E. Bergstrom, S. Fang, Y. Guan, K. Jennings, N. Gunaratna, Dyed microspheres for quantification of UV dose distributions: photo-chemical reactor characterization by Lagrangian Actinometry, *J. Environ. Eng. Sci.* 22 (2006) 615–628.
- [8] X. Zhao, S.M. Alpert, J.J. Ducoste, Assessing the impact of upstream hydraulics on the dose distribution of ultraviolet reactors using fluorescence microspheres and computational fluid dynamics, *Environ. Eng. Sci.* 26 (2009) 947–959.
- [9] K.P. Chiu, D.A. Lyn, P. Savoye, E.R. Blatchley III, Effect of UV system modification on disinfection performance, *J. Environ. Eng.* 125 (1999) 459–469.
- [10] A. Munoz, S. Craik, S. Kresta, Computational fluid dynamics for predicting performance of ultraviolet disinfection-sensitivity to particle tracking inputs, *J. Environ. Eng. Sci.* 6 (2007) 285–301.
- [11] C. Xu, X.S. Zhao, G.P. Rangaiah, Performance analysis of ultraviolet water disinfection reactors using computational fluid dynamics simulation, *Chem. Eng. J.* 221 (2013) 398–406.
- [12] C. Xu, G.P. Rangaiah, X.S. Zhao, A computational study of the effect of lamp arrangements on the performance of ultraviolet water disinfection reactors, *Chem. Eng. Sci.* 122 (2015) 299–306.
- [13] R. Sommer, A. Cabaj, T. Haider, G. Hirschmann, UV drinking water disinfection – requirements, testing and surveillance: exemplified by the Austrian National Standards M 5873-1 and M 5873-2, *IUVA News* 6 (2014), 4.
- [14] J.R. Taylor, *An Introduction to Error Analysis-Study of Uncertainty in Physical Measurement*, Oxford University Press, 1995.
- [15] G.D. Raithby, E.H. Chui, A finite-volume method for predicting a radiant heat transfer in enclosures with participating media, *J. Heat Transf.* 112 (1990) 415–423.
- [16] ANSYS, *ANSYS-FLUENT 12.0 Theory Guide*, 2012.
- [17] W.P. Jones, B.E. Launder, The prediction of laminarization with a two-equation model of turbulence, *Int. J. Heat Mass Transf.* 15 (1972) 301–314.
- [18] D.A. Sozzi, F. Taghipour, Computational and experimental study of annular photo-reactor hydrodynamics, *Int. J. Heat Fluid Flow* 27 (2006) 1043–1053.
- [19] S. Elyasi, F. Taghipour, Simulation of UV photoreactor for water disinfection in Eulerian framework, *Chem. Eng. Sci.* 61 (2006) 4741–4749.
- [20] D.A. Lyn, K. Chiu, E.R. Blatchley III, Numerical modeling of flow and disinfection in UV disinfection channels, *J. Environ. Eng.* 125 (1999) 17–26.
- [21] B.E. Launder, D.B. Spalding, *Lectures in Mathematical Models of Turbulence*, Academic Press, London, 1972.
- [22] P.A. Cundall, O.D.L. Strack, A discrete numerical model for granular assemblies, *Géotechnique* 29 (1979) 47–65.
- [23] S.A. Moris, A.J. Alexander, An investigation of particle trajectories in two-phase flow systems, *J. Fluid Mech.* 55 (1972) 193–208.
- [24] S.V. Patankar, *Numerical Heat Transfer and Fluid Flow*, Hemisphere Publisher, New York, 1980.
- [25] H.K. Versteeg, W. Malalasekera, *An Introduction to Computational Fluid Dynamics: The Finite Volume Method*, second ed., Prentice Education Limited, England, 2007.
- [26] A. Sozzi, F. Taghipour, Modeling the performance of ultraviolet reactor in Eulerian and Lagrangian frameworks, in: *Fifth International Conference on CFD in the Process Industries*, CSIRO, Melbourne, Australia, 2006.
- [27] D.I. Graham, R.A. Moyeed, How many particles for my Lagrangian simulations, *Powder Technol.* 125 (2002) 179–186.